ELSEVIER

European Journal of Cardio-thoracic Surgery 40 (2011) 322–327

EUROPEAN JOURNAL OF CARDIO-THORACIC SURGERY

www.elsevier.com/locate/ejcts

Winner of the EACTS Young Investigator Award 2010 - Category 'Thoracic'.

Novel approach for detection of isolated tumor cells in pulmonary vein using negative selection method: morphological classification and clinical implications☆,☆☆

Soichiro Funaki, Noriyoshi Sawabata*, Tomoyuki Nakagiri, Yasushi Shintani, Masayoshi Inoue, Yoshiki Kadota, Masato Minami, Meinoshin Okumura

Department of General Thoracic Surgery, Osaka University Graduate School of Medicine, Osaka, Japan

Received 10 August 2010; received in revised form 28 October 2010; accepted 4 November 2010; Available online 7 January 2011

Abstract

Objective: The presence of isolated tumor cells (ITCs) in the pulmonary vein (PV) of a lung resected for lung cancer has been reported to be a prognostic factor. Previous investigations noted correlations between prognosis and the presence or amount of ITCs, although few studies have investigated the clinical implications of the morphological characteristics of those cells. We assessed the clinical implications of ITCs in the PV using a novel enrichment approach that maintained their morphological characteristics. **Methods:** Ninety-four consecutive patients with primary non-small-cell lung cancer (NSCLC) without preoperative chemo- and/or radiation therapy (p-stage I in 75, II in 13, III or IV in six) were studied. Blood samples were drawn from the PV draining the lung just after pulmonary resection, and ITCs were enriched using a CD45-negative selection method and density-gradient centrifugation, followed by Papanicolaou staining using 1 ml of PV blood and immunohistochemical staining for cytokeratin in cases with an additional available blood sample. The ITCs were classified into four types based on patterns of cluster formation: no tumor cells (N), singular tumor cells (S), clustered cells (≤0.2 mm) (CSs), and bulky clustered cells (>0.2 mm) (BCSs). We evaluated the correlations between ITC morphology and clinical results. **Results:** ITCs were detected in 68 of 94 patients (72%), of which the BCS type was observed in two, CS in 33, S in 33, and N in 26. Over a median follow-up period of 13 months (range 6–22 months), cancer recurrence occurred in 16 cases (17%): 14 in the combined CS/BCS group, one in S, and one in N. Log-rank analysis revealed that the disease-free survival rate was exclusively worse in patients with clustered ITCs as compared with the other two groups ($p < 0.01$). **Conclusions:** The present method was useful to detect and enrich ITCs from the PV, and showed the clinical relevance of their morphology in lung cancer cases. The presence of ITC clusters may be a prognostic biomarker for patients with resected NSCLC.

Keywords: Lung cancer; Surgery; Isolated tumor cells; Morphology

1. Introduction

Primary lung cancer remains a leading cause of cancer death in most industrialized countries [1], with most cancer deaths related to high rates of recurrence and distant metastasis; thus, useful biomarkers are needed for early detection of both. Recently, isolated tumor cells (ITCs) in blood were reported to be useful markers for prognosis, recurrence, and metastasis [2]. It has been speculated that ITCs are likely shed from the primary tumor, then flow through a drainage vein and circulate throughout the body.

A number of methods to detect ITCs have been reported, with polymerase chain reaction (PCR)-based assays the most widely used [3], as a high sensitivity of ITC detection and clinical implications of the results have been shown [4–6]. Recently, the CellSearch® System (Veridex LLC, Rartian, NJ, USA) was shown to provide accurate detection and enrichment of rare ITCs from blood samples of patients with various types of solid cancer, including lung cancer [7], colon cancer [8], and breast cancer at the single cell level [9]. In addition,

☆ Presented at the 24th Annual Meeting of the European Association for Cardio-thoracic Surgery, Geneva, Switzerland, September 11–15, 2010.

☆☆ This research was supported by a Grant-in-Aid for Scientific Research (B) from the Japan Ministry of Education, Science, Sports and Culture, and the Uehara Memorial Foundation.

* Corresponding author. Address: Department of General Thoracic Surgery, Osaka University Graduate School of Medicine, L-5 2-2 Yamadaoka Suita-city, Osaka, 565-0897, Japan. Tel.: +81 6 6879 3152; fax: +81 6 857 3179.

E-mail addresses: sawabata@thoracic.med.osaka-u.ac.jp, nsawabata@hotmail.com (N. Sawabata).

1010-7940/$ – see front matter
doi:10.1016/j.ejcts.2010.11.029

associations between the number of ITCs with tumor stage and progression have been reported [10]. Most previous studies were quantitative investigations used to evaluate ITCs, and there are few reports of the clinical implication of ITCs that used morphological classification. We conducted the present investigation to assess the clinical implications and morphological characteristics of ITCs in the PV of resected lungs of non-small-cell lung cancer (NSCLC) patients using a novel approach for ITC enrichment and detection.

2. Patients and methods

2.1. Cell-spiking experiment

Initially, to evaluate the accuracy and sensitivity of our method to detect ITCs, a cell-spiking experiment was performed using two lung cancer cell lines, COR-L32 (human small-cell lung carcinoma; ATCC® Catalogue No. 96020744) and SK-LU-1 (human adenocarcinoma; ATCC® Catalogue No. HTB-57™), prior to the examination of clinical samples to detect ITCs in blood samples. The cell lines were maintained in Eagle's Minimum Essential Medium (EMEM) supplemented with fetal bovine serum (FBS) to a final concentration of 10% and incubated at 37 °C. After adding a known number of cells to 1-ml whole blood samples obtained from healthy volunteers, we assessed the sensitivity of our method by determining the ratio of the number of enriched cells to the number of added cells with a hemacytometer.

The method of cell extraction employed was as follows. A RosetteSep® Human CD45 Depletion Cocktail (Stemcell Technologies, Inc.) was added at 50 $\mu l\ ml^{-1}$ to individual whole blood samples and mixed well. After incubation for 20 min at room temperature, the mixture was diluted with an equal volume of phosphate-buffered saline + 2% fetal bovine serum (PBS + 2% FBS) and mixed gently. The diluted sample was then layered on top of a Ficoll-Paque™ PLUS and centrifuged for 20 min at 1200 × *g* at room temperature, with the brake in the off position; then, the enriched ITCs were removed from the Ficoll-Paque™ PLUS–plasma interface. After washing enriched ITCs with PBS + 2% FBS, the cells were centrifuged down to polylysine-coated glass slides using a cytospin device at 1000 × *g* for 3 min. Cells on the slides were stained using Papanicolaou stain and a cytokeratin immunohistochemistry kit (Carcinoma cell detection kit human, Miltenyi Biotec® Catalogue No. 130-090-463), which resulted in a cell collection ratio of 60% for both single cells and clustered cells. Tumor cells that existed among the total nuclear cell count ranged from 1×10^2 to 1×10^3 in number.

Table 1. Patient characteristics and distribution of isolated tumor cells in pulmonary venous blood.

	Total	PV cytology			*p*-Value
		N	S	C	
No.	94	26	33	35	
Gender					0.8
Male	56	17	19	20	
Female	38	9	14	15	
Age (mean ± SD)	67.7 ± 8.4	68.8 ± 8.3	67.2 ± 9.0	70.0 ± 10.9	0.5
<70	49	14	21	14	0.1
≥70	45	12	12	21	
pT factor					0.3
T1	52	18	19	15	
T2	36	7	12	17	
T3	6	1	2	3	
pN factor					1.0
N0	84	24	29	31	
N1	4	1	2	1	
N2	5	1	2	2	
NX	1	0	0	1	
pM factor					1.0
M0	93	26	33	34	
M1a	1	0	0	1	
M1b	0	0	0	0	
p-Stage					0.6
I	75	23	27	25	
II	13	2	4	7	
III or IV	6	1	2	3	
Tumor histology					0.9
Adenocarcinoma	71	19	26	26	
Squamous cell carcinoma	14	4	5	5	
Miscellaneous	9	3	2	4	
Tumor location					0.1
RU	44	13	13	18	
RM	3	0	3	0	
RL	13	2	6	5	
LU	23	4	9	10	
LL	11	7	2	2	

PV, pulmonary vein; N, no tumor cells; S, singular tumor cells; CS/BCS, clustered tumor cells; RU, right upper lobe; RM, right middle lobe; RL, right lower lobe; LU, left upper lobe; LL, left lower lobe.

2.2. Patients

Ninety-four consecutive patients (56 males, 38 females; range 28–88 years old, median 67.7 years) with primary NSCLC, who did not undergo preoperative chemo- and/or radiation therapy, were evaluated using our method (Table 1). Written informed consent was obtained from all patients enrolled. This study conformed to the ethical guidelines of Osaka University Graduate School of Medicine, and was approved by the institutional review board of Osaka University Medical Hospital. All patients underwent a segmentectomy ($n = 11$), lobectomy ($n = 80$), or bilobectomy ($n = 3$) with a systematic mediastinal lymphadenectomy from August 2008 to January 2010 at Osaka University Medical Hospital.

The postoperative staging of all patients was determined according to the tumor–node–metastasis (TNM) classification of the Union for International Cancer Control (UICC), ver. 7, 2009 (Table 1). The median follow-up duration was 13 months (6–22 months). In follow-up examinations, all patients were evaluated at 3-month intervals. Each evaluation included a physical examination, chest X-ray, and blood tests including tumor markers, while additional thoracic–abdominal computed tomography (CT) scans were generally performed at 6-month intervals.

2.3. Blood samples and ITC detection and enrichment

All blood samples were collected on the back table immediately after lung resection by gentle aspiration with an 18-gauge needle from the tumor-draining pulmonary vein (PV), which was stapled before the resection in all cases, and placed in 10-ml ethylene diamine tetraacetic acid (EDTA) tubes. ITCs were isolated using a negative selection method from 1-ml blood samples by the method described above. In addition, cytokeratin immunohistochemistry was performed, if an additional blood sample was available.

2.4. Evaluation and classification of clusters

Using all of the samples, one glass slide containing enriched ITCs from each patient was prepared and assessed by Papanicolaou staining. This examination was performed independently by two cytologists (E.Y and H.Y) who were unaware of the patient's clinical data. For morphological assessment, each cytologist distinguished cancer cells from normal cells by light microscopy based on their morphological appearance, such as cell size and shape, nuclear size and shape, and nuclear–cytoplasmic ratio (N/C). Furthermore, for cluster formation assessment, patterns of ITCs were classified into the following four types: no tumor cells (N), singular cells (S), clustered cells ($\leq$0.2 mm in size) (CSs) including singular cells, and bulky clustered cells (>0.2 mm in size) (BCSs), which included clustered cells and singular cells.

2.5. Statistical analysis

Statistical analysis was performed using the SPSS Exact Tests software. The Kruskal–Wallis test was used to calculate mean values, and prevalence was analyzed with Fisher's exact test. For analysis of follow-up data, survival curves were calculated with the Kaplan–Meier method and survival distributions were compared by a log-rank test. The Cox proportional hazards model was applied for calculating hazard ratio by uni- and multivariate analyses. The threshold for statistical significance was a p-value less than 0.05.

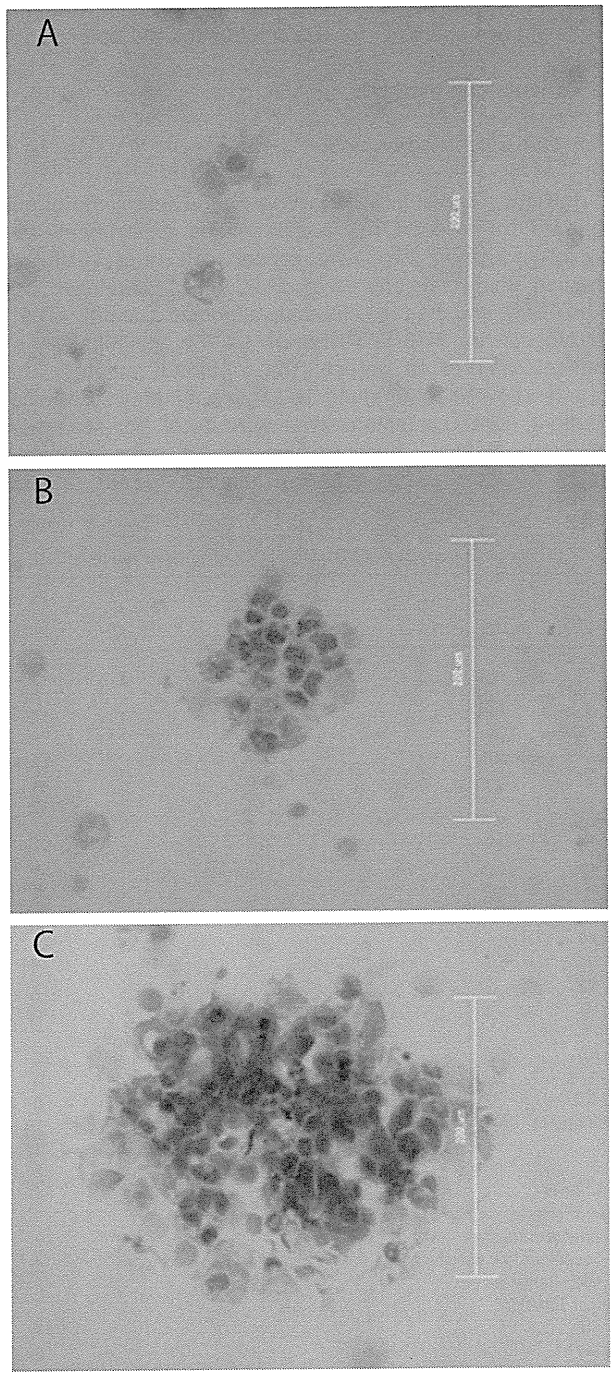

Fig. 1. Classification of isolated tumor cells by cluster formation. Shown are results following Papanicolaou staining. (A) Arrows indicate singular cancer cells. (B) Clustered cancer cells ($\leq$0.2 mm). (C) Bulky clustered cells (>0.2 mm). Original magnification ×40. Scale bars = 0.2 mm.

3. Results

3.1. Detection of ITCs

Using Papanicolaou staining, ITCs classified as S were detected in 33 (35%) of the 94 patients, while those classified as CS or BCS were found in 35 (37%). Fig. 1 shows examples of singular and cluster formations of CTCs. Cases classified as CS and BCS were considered as a single group for analysis of survival, as the number of BCS cases was small. Cytokeratin examinations were performed in 59 cases (15 classified as N, 21 as S, 22 as CS, and one as BCS). All cases classified as CS or BCS revealed positive results for cytokeratin staining, whereas only seven (33%) of those classified as S and none as N showed positive cytokeratin staining results.

3.2. ITC classification and prognosis

The correlations of patient characteristics with distribution of ITCs in pulmonary venous blood are shown in Table 1. There were no significant differences regarding patient characteristics among the three groups (N, S, and CS/BCS). Sixteen patients suffered cancer relapse, including 14 in the CS/BCS group, one in S, and one in N: these could be detailed as exclusive local recurrence in four (pleura in one, chest wall in one, hilar lymph node in one, mediastinal lymph node in one), local and distant metastasis in seven (bilateral lungs in four, mediastinal lymph node and neck lymph node in two, mediastinal lymph node and bone in one), and exclusive distant metastasis in five (contralateral lung in three, adrenal gland in one, and brain and liver in one). Relapse-free survival curves are shown in Fig. 2, which demonstrated that the cluster group (CS/BCS) exclusively was statistically significant; overall survival curves are shown in Fig. 3. Univariate analysis revealed that the presence of clustered ITCs and p-stage III or IV were significant prognostic factors in the analysis of disease-free survival, and those results were confirmed by multivariate analysis findings (Table 2).

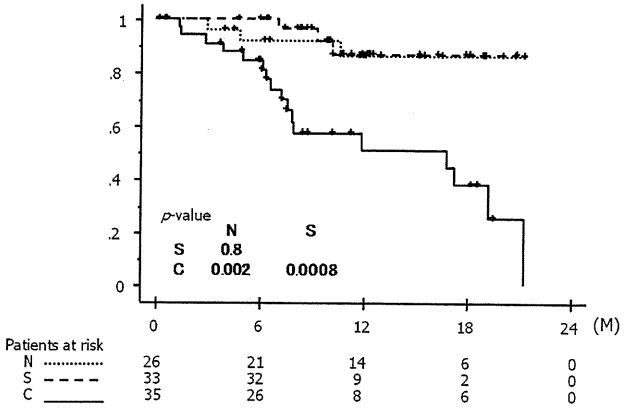

Fig. 2. Relapse-free survival curves.
N, patients with no tumor cells; S, patients with singular tumor cells; C, patients with clustered tumor cells (CS/BCS).

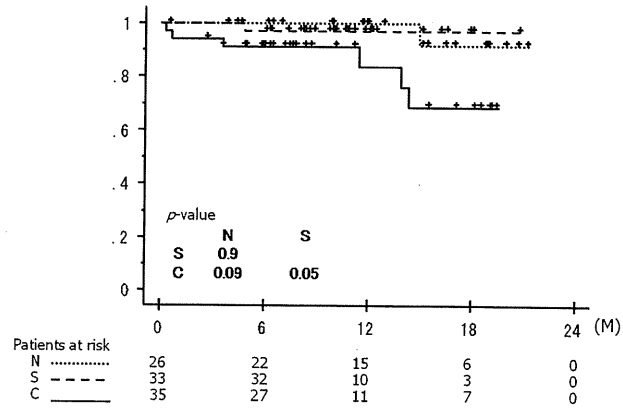

Fig. 3. Overall survival curves.
N, patients with no tumor cells; S, patients with singular tumor cells; C, patients with clustered tumor cells (CS/BCS).

4. Discussion

In the present study, we focused on the morphological appearance of ITCs and investigated related clinical implications. Our results showed that cluster formations of ITCs may be a prognostic indicator for early recurrence of lung cancer. In cases with singular cancer cells, the recurrence rate was low as compared with those with cluster formation. However, the clinical implications of the presence of singular ITCs remain unclear and a longer duration follow-up study is needed to determine clinical outcomes over a long period.

In spite of early discovery of cancer and complete surgical resection, the rates of recurrence and mortality in lung cancer cases remain high [1]. During treatment of postoperative patients, it is especially important to detect early relapse and distant metastasis. Thus, it is crucial to develop useful biomarkers for predicting early recurrence and metastasis. Some recent studies have demonstrated that the presence of ITCs in circulating blood was useful as a biomarker for the prognosis of various types of disease, such as breast cancer [7], colorectal cancer [6], and lung cancer [11].

Various methods to detect and enrich ITCs have been reported. In older studies, ITCs were observed using whole blood samples [12], though those results are not considered to be reliable. Recently, Sienel et al. used a cytokeratin immunohistochemistry method to reveal that the presence of ITCs in samples collected from the PV of a pulmonary lobe containing lung cancer before resection was a predictor of poor survival [13]. In addition, Yamashita et al. reported a study that used reverse transcriptase-polymerase chain reaction (RT-PCR) assays of peripheral blood to detect messenger RNA (mRNA) of carcinoembryonic antigen (CEA), and noted that its presence was a prognostic indicator in patients with NSCLC [11]. Current advancement in technology allow for ITCs to be captured and quantitatively evaluated with the semi-automated CellSearch® System (Veridex LLC, NJ, USA). Using this system, some groups have reported that determination of the number of pre- and postoperative ITCs was useful as a biomarker for survival and prognosis [7,10], while another showed that those results were able to reveal cancer cell spreading caused by the operation [14]. However, most of those studies used

Table 2. Results of univariate and multivariate analyses of relapse-free survival.

Variables	Univariate			Multivariate		
	R.R.	95% C.I.	*p*-Value	R.R.	95% C.I.	*p*-Value
ITCs in PV						
None	Ref.			Ref.		
Singular	0.901	0.180–4.505	0.9	0.845	0.170–4.577	0.9
Clustered	5.894	1.717–20.23	0.005	8.882	1.676–21.04	0.006
Gender						
Male	Ref.					
Female	0.882	0.355–1.904	0.7	0.895	0.319–2.515	0.8
Age in years						
<70	Ref.					
≥70	1.923	0.831–4.446	0.1	1.279	0.490–3.339	0.6
p-Stage						
I	Ref.					
II	2.122	0.686–6.557	0.2	2.096	0.588–7.474	0.3
III or IV	7.591	2.612–22.06	0.0002	9.756	3.357–40.37	0.002
Tumor histology						
Adenocarcinoma	Ref.					
Squamous cell carcinoma	1.717	0.560–5.265	0.3	2.147	0.588–7.847	0.2
Miscellaneous	2.456	0.806–7.482	0.1	1.081	0.225–5.204	0.9

quantitative evaluation methods and few have shown the significance of qualitative evaluation of ITCs.

In the present study, early relapse was associated with the presence of clustered cancer cells. We speculated that cancer cells may be able to live for a longer period in circulating blood when clustered, thus allowing direct access to distant organs and easy establishment of a secondary tumor. In addition, when considering tumor-initiating cells, it is possible that cells with a large diameter have a greater potential of causing relapse [15].

A recent study noted that epithelial–mesenchymal transition (EMT) plays important roles in cancer progression and metastasis [16]. Through the EMT process, the morphology and gene expression of the epithelial markers E-cadherin and cytokeratin become altered in cancer cells [17,18]. Our present analysis using immunohistochemical staining for cytokeratin showed that the positive rate of CS/BCS cases was 100%, whereas that in cases classified as S was low (33%). The reason for the different rates of positivity between S and CS/BCS cases may be related to EMT. Furthermore, the low occurrence of cytokeratin staining in cases classified as S may indicate that the expression of cytokeratin was reduced during the EMT process.

There are some limitations to our method, as accurate cell counting and ITC enrichment have not been perfected. On the other hand, with the CellSearch® system [7–10], cell-number counting and enrichment are easily performed in a semiautomatic fashion, though it is difficult to detect morphological features, in contrast to the method used in the present study. Moreover, there are problems with the procedure used to collect the samples. In the present method, in patients, after resecting the lung and placing it on the back table, blood was collected by aspiration from the PV, which had been stapled before the resection. Ideally, blood samples should be collected from the PV with proximal clamping before lung resection. In addition, it would be good to perform the assays with blood samples obtained from the peripheral vein. Some studies have presented preoperative and postoperative analyses of ITCs obtained from peripheral blood samples [7,11]. In the future, we intend to collect blood samples before lung resection and perform the assays using peripheral blood samples. In addition, we hope to conduct additional research using blood samples obtained at various time points before, during, and after surgery.

In conclusion, the present CD45-negative selection method was found useful to detect and enrich ITCs from blood samples obtained from the PV of lungs resected for NSCLC. In addition, our results show the clinical relevance of morphological classification of ITCs in NSCLC cases, as the presence of clustered ITCs was a prognostic indicator for patients following surgical resection.

Acknowledgments

The authors thank Professor Katsuyuki Aozasa, Dr Eiichi Morii, and Dr Hideo Yoshimura (Department of Pathology, Osaka University Graduate School of Medicine) for their contributions to the cytological diagnosis.

References

[1] Alberg AJ, Ford JG, Samet JM. American College of Chest Physicians. Epidemiology of lung cancer: ACCP evidence-based clinical practice guidelines (2nd edition). Chest 2007;132:29S–55S.

[2] Pantel K, Brakenhoff RH, Brandt B. Detection, clinical relevance and specific biological properties of disseminating tumour cells. Nat Rev Cancer 2008;8:329–40.

[3] Smith B, Selby P, Southgate J, Pittman K, Bradley C, Blair GE. Detection of melanoma cells in peripheral blood by means of reverse transcriptase and polymerase chain reaction. Lancet 1991;338:1227–9.

[4] Kurusu Y, Yamashita J, Ogawa M. Detection of circulating tumor cells by reverse transcriptase-polymerase chain reaction in patients with resectable non-small-cell lung cancer. Surgery 1999;126:827–8.

[5] Iinuma H, Okinaga K, Egami H, Mimori K, Hayashi N, Nishida K, Adachi M, Mori M, Sasako M. Usefulness and clinical significance of quantitative real-time RT-PCR to detect isolated tumor cells in the peripheral blood and tumor drainage blood of patients with colorectal cancer. Int J Oncol 2006;28:297–306.

[6] Ignatiadis M, Xenidis N, Perraki M, Apostolaki S, Politaki E, Kafousi M, Stathopoulos EN, Stathopoulou A, Lianidou E, Chlouverakis G, Sotiriou C, Georgoulias V, Mavroudis D. Different prognostic value of cytokeratin 19 mRNA positive circulating tumor cells according to estrogen receptor and HER2 status in early-stage breast cancer. J Clin Oncol 2007;25:5194–202.

[7] Okumura Y, Tanaka F, Yoneda K, Hashimoto M, Takuwa T, Kondo N, Hasegawa S. Circulating tumor cells in pulmonary venous blood of primary lung cancer patients. Ann Thorac Surg 2009;87:1669–75.

[8] Sastre J, Maestro ML, Puente J, Veganzones S, Alfonso R, Rafael S, Garcia-Saenz JA, Vidaurreta M, Martin M, Arroyo M, Sanz-Casla MT, Diaz-Rubio E. Circulating tumor cells in colorectal cancer: correlation with clinical and pathological variables. Ann Oncol 2008;19:935–8.
[9] Cristofanilli M, Budd GT, Ellis MJ, Stopeck A, Matera J, Miller MC, Reuben JM, Doyle GV, Allard WJ, Terstappen LW, Hayes DF. Circulating tumor cells, disease progression, and survival in metastatic breast cancer. N Engl J Med 2004;351:781–91.
[10] Tanaka F, Yoneda K, Kondo N, Hashimoto M, Takuwa T, Matsumoto S, Okumura Y, Rahman S, Tsubota N, Tsujimura T, Kuribayashi K, Fukuoka K, Nakano T, Hasegawa S. Circulating tumor cell as a diagnostic marker in primary lung cancer. Clin Cancer Res 2009;15:6980–6.
[11] Yamashita J, Matsuo A, Kurusu Y, Saishoji T, Hayashi N, Ogawa M. Preoperative evidence of circulating tumor cells by means of reverse transcriptase-polymerase chain reaction for carcinoembryonic antigen messenger RNA is an independent predictor of survival in non-small cell lung cancer: a prospective study. J Thorac Cardiovasc Surg 2002;124:299–305.
[12] Stuart R, Alvin W, Ruth M, Elizabeth M, Warren C. Technique and results of isolation of cancer cells from the circulating blood. AMA Arch of Surg 1958;76:334–46.
[13] Sienel W, Seen-Hibler R, Mutschler W, Pantel K, Passlick B. Tumour cells in the tumour draining vein of patients with non-small cell lung cancer: detection rate and clinical significance. Eur J Cardiothorac Surg 2003;23:451–6.
[14] Sawabata N, Okumura M, Utsumi T, Inoue M, Shiono H, Minami M, Nishida T, Sawa Y. Circulating tumor cells in peripheral blood caused by surgical manipulation of non-small-cell lung cancer: pilot study using an immunocytology method. Gen Thorac Cardiovasc Surg 2007;55:189–92.
[15] Liotta LA, Kleinerman J, Saidel GM. Quantitative relationships of intravascular tumor cells, tumor vessels, and pulmonary metastases following tumor implantation. Cancer Res 1974;34:997–1004.
[16] Thiery JP, Acloque H, Huang RY, Nieto MA. Epithelial-mesenchymal transitions in development and disease. Cell 2009;139:871–90.
[17] Tsuji T, Ibaragi S, Hu GF. Epithelial-mesenchymal transition and cell cooperativity in metastasis. Cancer Res 2009;69:7135–9.
[18] Koo V, El Mekabaty A, Hamilton P, Maxwell P, Sharaf O, Diamond J, Watson J, Williamson K. Novel in vitro assays for the characterization of EMT in tumourigenesis. Cell Oncol 2010;32:67–76.

Appendix A. Conference discussion

Dr G. Varela *(Salamanca, Spain)*: To my knowledge, you are the first to demonstrate that the presence of clusters of tumor cells in pulmonary venous blood adversely influences the prognosis in pathological stage I non-small cell lung cancer cases.

Previously, different authors have reported the finding of epithelial cells in blood obtained from pulmonary veins after lung resection by means of antibodies against the epithelial cell adhesion molecule using the so-called Cell Search System. According to Passlick, this happens in less than 20% of the resected cases, while Okumura and co-workers reported circulating tumor cells in more than 95% of their cases. With your technique you have detected clusters of tumor cells in around 30% of your cases. This seems to be more specific for tumor cell detection and also more sensitive than simple immunohistochemical staining. I'm wondering if this 30% prevalence of clusters of cells may be related to anatomical conditions or to the type of surgical techniques; for instance, the tumor size or location in the lobe, the way of handling the tumor during surgery, the sequence of vessel ligation and so on.

My second question is, if the finding of clusters of cells is not related to surgical manipulation, maybe comparable findings could be elicited in sequentially-taken samples of peripheral arterial blood prior to surgery, indicating the need for induction chemotherapy even in selected clinical stage IA cases. Do you have any preliminary data on this or are you thinking about a similar study?

Dr Funaki: As you mentioned, I think surgical manipulation is an important problem. I think surgical manipulation may enhance the cancer cells shedding into the bloodstream, as you mentioned, but I don't think that all cancer cells are shed into the bloodstream only by surgical manipulation.

As for the surgical techniques, in our research we first ligate the pulmonary vein. So there is the possibility that surgical manipulation may enhance cancer cells shedding in the bloodstream and that the number of isolated tumor cells may increase.

doi:10.1510/icvts.2010.249896

INTERACTIVE CARDIOVASCULAR AND THORACIC SURGERY

Interactive CardioVascular and Thoracic Surgery 12 (2011) 733-738

www.icvts.org

Institutional report - Thoracic oncologic

Validation of pN2 sub-classifications in patients with pathological stage IIIA N2 non-small cell lung cancer

Tomoyuki Nakagiri, Noriyoshi Sawabata*, Souichirou Funaki, Masayoshi Inoue, Yoshihisa Kadota, Yasushi Shintani, Meinoshin Okumura

Department of General Thoracic Surgery, Osaka University Graduate School of Medicine, 2-2 (L5) Yamadaoka, Suita City, Osaka 565-0871, Japan

Received 2 August 2010; received in revised form 16 November 2010; accepted 24 November 2010

Institutional Report

Abstract

Optimal surgical treatment for patients with stage IIIA N2 non-small cell lung cancer (NSCLC) remains a matter of debate, because of the outcomes. The outcomes may be affected from variations in patterns of lymph node metastasis. As the patterns of lymph node sub-classifications, multiple station metastases of mediastinal lymph nodes (MN2), highest metastasis of the mediastinal lymph nodes (HM), distribution of metastatic nodes (skip N2 or non-skip N2), and clinical (c-) N factor have been cited. We investigated these factors for patients with pathological stage IIIA (pIIIA) N2 NSCLC. We reviewed 121 consecutive patients with pIIIA N2 who underwent complete resection. Age, gender, tumor laterality, histology, lobe location of the tumor, c-T factor, pathological (p-) T factor, c-N factor, MN2, HM and skip N2 condition were used as prognostic variables. Overall five-year survival rate was 41.8%. Based on log-rank testing, c-T factor ($P=0.022$), p-T factor ($P=0.0002$), c-N factor ($P=0.009$), HM ($P=0.019$) and skip N2 ($P=0.030$) were identified as significantly prognostic. Using these variables, p-T factor, c-N factor and skip N2 showed significance and independence on Cox multivariate analysis. The sub-classification of lymph node metastasis in patients with p-stage IIIA N2 NSCLC has clinical implications for the prognosis.

Keywords: Stage IIIA; Lung cancer; Lymph node metastasis sub-classification; skip N2; Multiple station N2; Highest metastasis; Clinical N factor

1. Introduction

Studies have reported varying prognosis for patients with pathological N2 (pN2) stage IIIA non-small cell lung cancer (NSCLC), with five-year survival rates (5YSRs) ranging between 25% and 50% [1–3]. One of the reasons for this variance in 5YSR may come from differences in the pattern of lymph node metastasis in pathological stage IIIA N2 disease. Some studies have reported that single or multiple N2 disease and clinical N (c-N) factor are prognostic factors [1–3]. Another study has reported that when positive results were seen for the highest mediastinal lymph node, meaning the dissected mediastinal lymph node occupying the position closest to the head, outcomes were worse than in patients in which the highest node was negative [1]. Distribution of metastatic nodes (skip N2 or non-skip N2, meaning the absence or presence of N1 disease in patients with N2 metastasis or presence of N1 disease of such patients) has also been reported as a prognostic factor [4]. We retrospectively investigated these factors in the cohort of our single institute experience, and examined the clinical validity of the lymph node metastasis sub-classification.

*Corresponding author. Tel.: +81-6-6879-3152; fax: +81-6-6879-3164.
E-mail address: sawabata@thoracic.med.osaka-u.ac.jp (N. Sawabata).

2. Patients and methods

2.1. Patients

Between January 1992 and July 2007, 938 patients underwent surgical resection for NSCLC that were performed at Osaka University Hospital. Of these, subjects comprised 121 consecutive patients with NSCLC pathological stage IIIA N2, who underwent surgically complete resection (12.9% of all surgical resection for NSCLC, Table 1).

Lymph nodes were dissected as ND2a, which included hilar and mediastinal lymph nodes, as described elsewhere [5]. Preoperative diagnoses of lymph node metastasis were performed using computed tomography (CT) and fluorodeoxyglucose-positron emission tomography (FDG-PET). Mediastinal lymph nodes with a short axis >1 cm on CT and/or positive uptake on FDG-PET were regarded as infiltrated lymph nodes. Brain CT or magnetic resonance imaging, upper abdominal CT and bone scintigraphy were performed to detect distant metastasis. Postoperative staging was performed according to version 6 of the International Union Against Cancer TNM classification (1997) [6]. Dissected lymph nodes were classified using Naruke's numbering system [7]. In the cohort, there were 3 c-N3 patients. Two of them were diagnosed as N3-negative patients with mediastinoscopy for the uptake in the contralateral level #4 lymph node on FDG-PET. The other c-N3

Table 1. Characteristics of 124 patients

Age (years)	38–79 (median 65)
Gender	
Male	79
Female	42
Laterality	
Right	73
Left	48
c-Stage	
c-Stage IA	31
c-Stage IB	22
c-Stage IIA	5
c-Stage IIB	23
c-Stage IIIA	34
c-Stage IIIB	6
Largest tumor diameters	12–110 (median 32)
c-T factor	
c-T1	51
c-T2	56
c-T3–4	14
p-T factor	
p-T1	39
p-T2	71
p-T3	12
Histology	
Adenocarcinoma	80
Squamous cell carcinoma	30
Adenosquamous cell carcinoma	3
Large cell carcinoma	5
Others	3
Treatment	
Surgery alone	63
Surgery + chemotherapy	43
Surgery + radiation therapy	8
Surgery + chemo-radiation therapy (Induction therapy 13)	7
Operation procedure	
Pneumonectomy	8
Bilobectomy	10
Lobectomy	103

patient had a finding of FDG-PET uptake in the supraclavicular lymph node. However, the lymph node could have the uptake because of tuberculosis from his past history. The patient underwent mediastinal lymph node dissection before lobectomy. The peratracheal lymph nodes were diagnosed as no metastasis from frozen section.

To determine prognostic factors with patient death as an end-point, patients were evaluated on the basis of age, gender, tumor laterality (right or left), largest tumor diameter, clinical (c-) T factor, pathological (p-) T factor, histology, serum CEA level, c-N factor, number of metastatic mediastinal lymph nodes (single or multiple), highest mediastinal lymph node status, distribution of metastatic lymph nodes (skip N2 or non-skip N2), and induction/adjuvant therapy. Items in the sub-classifications of lymph node metastasis are shown in Table 2. In addition, the sub-classifications of lymph node metastasis and lung cancer recurrence rate were also compared.

2.2. Statistical analysis

Kaplan–Meier analyses and log-rank testing were applied for survival curves/disease-free survival curves and their comparisons, respectively, for c-T factors, c-N factors, c-stages, tumor laterality, induction/adjuvant therapy, histological types, p-T factors, and lymph node metastatic sub-classifications. In addition, the value from log-rank testing can be treated as an approximate value for generalized Mantel extension analysis. Therefore, log-rank tests were also applied as a test of survival curve uniformity for ≥ 3 groups [8]. Cox proportional hazards regression modeling was applied to analyze the prognostic influence of variables on survival for the same items. Statistical calculations were performed using StatView version 5.0 software (Abacus Concepts, Berkeley, CA, USA), and values of $P \leq 0.05$ were considered statistically significant.

3. Results

Overall 5YSR for the patients with p-stage IIIA N2 NSCLC, who underwent surgically complete resection, was 41.8%. Follow-up was completed in 78 patients, and median follow-up for all patients was 67.7 months (range, 2–210 months). Induction and adjuvant chemotherapy were performed in 13 and 28 patients, respectively. Induction and adjuvant radiation therapy were performed in three and nine patients, respectively. Preoperative serum CEA level was measured in 111 patients.

3.1. Preoperative diagnostic factors

The 5YSRs for patients and the results of log-rank test are listed in Table 3. The 5YSRs for patients with c-T1, c-T2, and c-T3–4 disease were 43.3%, 48.6% and 10.3%, respectively ($P=0.023$). According to P-values, groups were re-classified into two categories: c-T1–2 and c-T3–4. Survival was significantly better for c-T1–2 disease than for c-T3–4 ($P=0.022$, Table 3).

The 5YSRs for patients with c-N0, c-N1, and c-N2–3 disease were 52.0%, 41.4% and 29.5%, respectively ($P=0.028$, Fig. 1a). Again according to P-values, groups were re-classified into two categories: c-N0–1 and c-N2–3. Survival was significantly better for c-N0–1 disease than for c-N2–3 ($P=0.009$, Table 3). In addition, survival was significantly better for non-induction chemotherapy group than for chemotherapy group ($P=0.014$, Table 3).

Table 2. Sub-classification of lymph node metastases

c-N factor	
c-N0	56
c-N1	25
c-N2	37
c-N3	3
Metastatic lymph node number in N2 area	
Single	60
Multiple	57
Unknown	4
Highest lymph node status	
Positive	73
Negative	44
Unknown	4
Distribution of metastasis nodes	
Skip N2	43
Non-skip N2	74
Unknown	4

Table 3. Log-rank test

Variables	5YSR (%)	*P*-value	Re-classification[1]	5YSR[2] (%)	*P*-value
Preoperative factors					
c-T factor		0.023			0.022
c-T1	43.3		c-T1–2	46.5	
c-T2	48.6		c-T3–4	10.3	
c-T3–4	10.3				
c-N factor		0.028			0.009
c-N0	52.0		c-N0–1	48.4	
c-N1	41.4		c-N2–3	29.5	
c-N2–3	29.5				
c-Stage factor		0.221			
c-Stage IA	53.9				
c-Stage IB	60.4				
c-Stage IIA	30.0				
c-Stage IIB	38.5				
c-Stage IIIA	45.3				
c-Stage IIIB	0.0				
Laterality		0.191			
Left	30.8				
Right	51.3				
Histology		0.599			
Adeno	41.4				
Sq	42.6				
Others	44.4				
Serum CEA level		0.139			
Normal	55.7				
High	40.9				
Induction therapy		0.014			
Yes	12.7				
No	45.6				
Postoperative factors					
p-T factor		0.0007			0.0002
p-T1	47.0		p-T1–2	48.6	
p-T2	49.1		p-T3	0.0	
p-T3	0.0				
Adjuvant therapy		0.773			
Yes	43.5				
No	41.3				
Highest lymph node status		0.019			
Positive	34.7				
Negative	52.6				
Distribution of metastasis nodes		0.030			
Skip N2	48.2				
Non-skip N2	40.2				
Metastatic node station number		0.131			
Single	45.5				
Multiple	38.5				

[1]Re-classification: according to the log-rank test, the cohort was re-classified into two groups from three groups (see 'Statistical analysis' part of the main text). [2]5YSR, 5YSR after re-classification. 5YSR, 5-year survival rate; Adeno, adenocarcinoma; Sq, squamous cell carcinoma.

3.2. Postoperative diagnostic factors

The 5YSRs for patients with p-T1, p-T2, and p-T3 disease were 47.0%, 49.1% and 0.0%, respectively ($P=0.0007$). According to *P*-values, groups were re-classified into two categories: p-T1–2 and p-T3. Significant differences in survival were identified between patients with p-T1–2 and p-T3 ($P=0.0002$, Table 3).

The 5YSRs for patients with the highest mediastinal lymph node metastasis and patients with negative lymph nodes were 34.7% and 52.6%, respectively ($P=0.019$, Fig. 1b, Table 3). The 5YSRs for patients with skip N2 and non-skip N2 were 48.2% and 40.2%, respectively ($P=0.030$, Fig. 1c, Table 3). The 5YSRs for patients with single N2 and multiple N2 were 45.5% and 38.5%, respectively. No significant difference in survival was apparent between patients with single station N2 and multiple station N2, but the difference tended to be marked ($P=0.131$, Fig. 1d, Table 3).

3.3. Cox proportional hazards regression model analyses

According to log-rank test results, c-N factor and p-T factor were re-classified into two categories each. In addition, histopathological subtype showed a multi-colinearity to patient survival in multiple linear regression analysis. These items were therefore omitted from analysis. Univariate analysis using the variables listed in Table 4 showed c-N factor, induction therapy, p-T factor and highest lymph node metastasis as significant prognostic factor. Distribution of metastatic lymph nodes (skip N2 or non-skip N2) was not a significant factor, but showed a tendency toward being a prognostic factor.

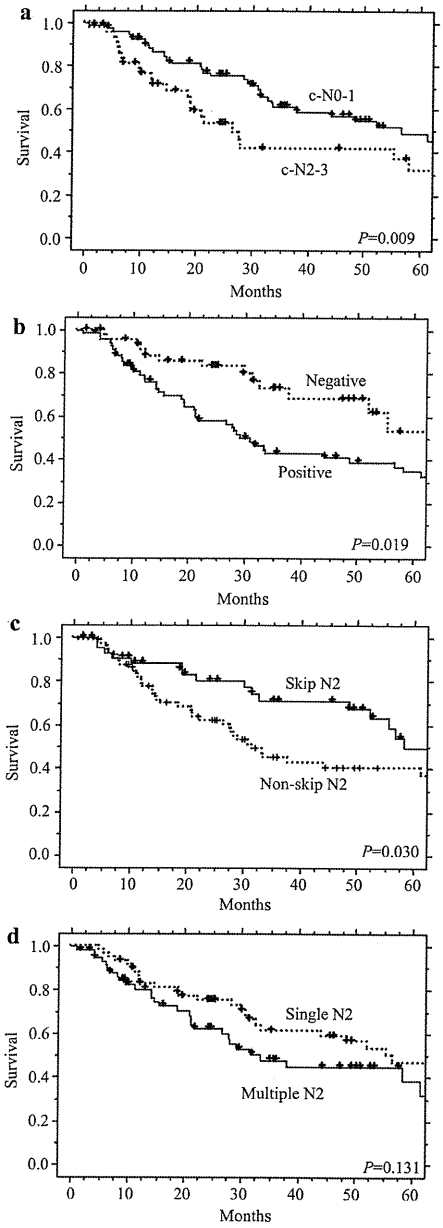

Fig. 1. (a) Probability of survival for patients with stage IIIA N2 NSCLC who underwent complete resection according to clinical N (c-N) factor. The five-year survival rates were 48.4% for cN0–1 and 29.5% for cN2–3. A significant difference in survival was apparent between patients with c-N0–1 and patients with c-N2–3 ($P=0.009$). (b) Probability of survival for patients with stage IIIA N2 NSCLC who underwent complete resection according to highest lymph node infiltration (HM). The five-year survival rates were 34.7% for positive infiltration and 52.6% for negative infiltration. A significant difference in survival was seen between patients with positive HM and those with negative HM ($P=0.019$). (c) Probability of survival for patients with stage IIIA N2 NSCLC who underwent complete resection according to distribution of metastasis node (skip N2 or non-skip N2). The five-year survival rates were 48.2% for skip N2 and 40.2% for non-skip N2. A significant difference in survival was apparent between patients with skip N2 and those with non-skip N2 ($P=0.030$). (d) Probability of survival for patients with stage IIIA N2 NSCLC who underwent complete resection according to the number of metastatic node stations (single N2 or multiple N2). The five-year survival rates were 45.5% for single station N2 and 38.5% for multiple station N2. Unfortunately, no significant difference in survival was seen between patients with single station N2 and those with multiple station N2 ($P=0.131$).

For multivariate analysis, there are strong correlations between c-N factor and induction therapy, and between c-N factor and metastatic lymph node number. Therefore, only c-N factor was analyzed among them (Table 4). We found c-N factor and p-T factor as independent prognostic factors. In addition, distribution of metastatic lymph nodes had a tendency of independence of prognostic factor.

3.4. Recurrence and the sub-classifications of lymph node metastasis

The recurrence status of lung cancer could be identified in 98 patients and the sub-classification status was unknown in two of them. There were significant differences among the disease-free survivals in the sub-classification statuses (Table 5). The five-year disease-free survival rates for patients with the highest mediastinal lymph node metastasis and patients with negative lymph nodes were 21.1% and 41.2%, respectively ($P=0.029$). The five-year disease-free survival rates for patients with skip N2 and non-skip N2 were 47.3% and 18.7%, respectively ($P=0.007$). The five-year disease-free survival rates for patients with single N2 and multiple N2 were 40.0% and 19.4%, respectively ($P=0.025$). The five-year disease-free survival rates for patients with c-N0–1 and c-N2–3 were 35.6% and 16.6%, respectively. No significant difference in disease-free survival was apparent between patients with c-N0–1 and c-N2–3, but the difference tended to be marked ($P=0.101$).

4. Discussion

Previous studies have revealed tumor laterality, lobe location of the tumor, histological type, T factor, number of metastatic mediastinal lymph nodes, highest mediastinal lymph node status and distribution of metastatic lymph nodes as prognostic factors for patients with stage IIIA N2 NSCLC after complete resection [1–3].

In the present analyses of preoperative diagnostic factors, a significant difference was seen between c-T1–2 and others. Similar findings were identified for p-T factor. The behavior of T1 and T2 was similar, as was the case for T3 and T4 disease. This result agrees with other previous data [3]. A significant difference was apparent between c-N0–1 and c-N2–3. Lymph node size according to CT is reportedly unreliable for evaluating metastasis [9]. However, many previous studies have reported significant associations with survival for clinical N factors in patients with stage IIIA NSCLC [1–3]. The results described by Prenzel et al. suggested difficulty in defining cut-off values to diagnose metastasis, and also showed a significant difference between the size of non-metastatic lymph nodes and size of infiltrated nodes [9]. Considering the results for c-T factor and c-N factor, clinical stage IIA NSCLC or earlier clinical stage NSCLC would represent good indications for surgical resection; even patients with pathological stage IIIA N2 NSCLC after operation may be suitable.

The survival of non-induction chemotherapy group was significantly better than that of induction therapy group in our cohort. Previous studies reported that induction chemotherapy is a recommendable therapy for stage IIIA N2 NSCLC [10, 11]. Our induction chemotherapy cohort had an

Table 4. Cox proportional hazards regression model analyses

Variables	Univariate analysis		*P*-value	Multivariate analysis		*P*-value
	HR	95% CI		HR	95% CI	
Age	1.03	0.99–1.06	0.11	1.03	0.99–1.07	0.08[1]
Gender (female/male)	0.86	0.50–1.50	0.60	0.87	0.43–1.80	0.71
c-N factors			0.02[2]			0.005[2]
c-N0–1	1			1		
c-N2–3	1.99	1.17–3.39		2.57	1.33–4.98	
Laterality (Lt/Rt)	1.41	0.84–2.38	0.19	0.90	0.46–1.76	0.77
Location			0.80			0.75
Upper lobe	1			1		
Middle lobe	1.08	0.42–2.77		0.65	0.20–2.11	
Lower lobe	0.84	0.47–1.50		0.88	0.46–1.76	
Pathology			0.60			0.54
Adeno	1			1		
Sq	0.88	0.47–1.66		0.63	0.27–1.46	
Others	1.50	0.59–3.87		0.73	0.20–2.73	
Serum CEA level			0.14			0.38
Normal	1			1		
High	1.53	0.87–2.71		1.35	0.69–2.65	
Induction therapy			0.007[2]			
Yes	2.60	1.20–5.19				
No	1					
p-T factors			<0.001[2]			0.004[2]
p-T1–2	1			1		
p-T3	3.32	1.71–6.48		3.77	1.53–9.24	
Highest						
Metastasis (+/−)	2.05	1.11–3.77	0.02[2]	1.75	0.85–3.60	0.13
Skip N2 (+/−)	0.62	0.35–1.10	0.10[1]	0.47	0.21–1.03	0.06[1]
Single N2 (m/s)	1.51	0.88–2.57	0.13			
Adjuvant therapy			0.44			0.81
Yes	0.81	0.73–2.09		0.92	0.48–1.76	
No	1			1		

[1]$P \leq 0.10$. [2]$P \leq 0.05$. HR, hazard ratio; CI, confidence interval; Adeno, adenocarcinoma; Sq, squamous cell carcinoma; m/s, multiple/single.

indication bias that induction chemotherapy was performed in clinically advanced cases. The bias may affect this result.

In the analyses of postoperative diagnostic factors, a significant difference was seen between pathological T3 and others. Significant differences in survival were also seen according to lymph node sub-classifications. A previous study reported highest mediastinal lymph node involvement as prognostic of highly advanced N2 disease resulting in poor outcomes [1]. Highest lymph node involvement could mean that surgery is more likely to be pathologically incomplete. Miyamoto et al. reported that 80% of patients with highest lymph node involvement showed neck lymph node metastasis [12]. Our result may support this finding. The prognosis of patients with highest lymph node involvement appears poor after surgery. Other studies have reported that non-skip N2 and multiple N2 are also prognostic for poor outcome [4]. The prognostic difference between skip N2 and non-skip N2 can be explained by the anatomic consideration that two separate lymph channels reach the mediastinal lymph nodes: one directly connected to the mediastinal lymph nodes and the other connected through the N1 lymph nodes to the mediastinal lymph nodes [13]. Skip N2 cases show involvement of only the former channel. In contrast, non-skip N2 could display the involvement of both channels. In this context, the difference between skip N2 and non-skip N2 may mean the same as the difference between single station N2 and multiple station N2. In addition, the recurrence rates of lung cancer had correlations with the sub-classification of the lymph node metastasis. The disease-free survival analysis showed also significant difference among the patients in the sub-classifications of lymph node metastasis. Recently, some investigation also presented that clinical N2 status and number of metastatic stations are prognostic factors for patients with p-stage IIIA N2 NSCLC [10, 11, 14]. Considering our results and the previous investigations, sub-classifications of mediastinal lymph node metastasis would have clinical implications on prognosis for patients with p-stage IIIA N2 NSCLC. In addition, the significance of systematic nodal dissection remains controversial [15]. However, from the current results and previous reports, systematic nodal

Table 5. Log-rank test for recurrence of lung cancer in the sub-classifications of lymph node metastasis

Variables	5-year survival rate (%)	*P*-value
c-N factor		0.101
c-N0–1	35.6	
c-N2–3	16.6	
Highest lymph node status		0.029
Positive	21.1	
Negative	41.2	
Distribution of metastasis nodes		0.007
Skip N2	47.3	
Non-skip N2	18.7	
Metastatic node station number		0.025
Single	40.0	
Multiple	19.4	

resection may have a somewhat different meaning for prognostic diagnosis in patients.

This investigation showed some limitations that require consideration, particularly the retrospective nature of the observation and the limited sample size. To clarify the clinical implications of p-N2 sub-classifications, which were speculated to be significant in this study, further studies using prospective cohorts are warranted.

5. Conclusion

This study revealed the sub-classifications of mediastinal lymph node metastasis, clinical N factor and distribution of metastatic lymph node, have clinical implications for the prognosis of patients with p-stage IIIA N2 NSCLC. In addition, patients with clinical stage IIA or earlier clinical stage NSCLC would be good candidates for pulmonary resection, and even patients with pathological stage IIIA N2 NSCLC may be suitable.

Acknowledgement

We thank Yuko Ohno of the Department of Health Promotion Science, Osaka University Graduate School of Medicine, Division of Health Sciences, for critical review of the manuscript and advice on statistical issues.

References

[1] Sakao Y, Miyamoto H, Yamazaki A, Oh T, Fukai R, Shiomi K, Saito Y. Prognostic significance of metastasis to the highest mediastinal lymph node in non-small lung cancer. Ann Thorac Surg 2006;81:292–297.
[2] Inoue M, Sawabata N, Takeda S, Ohta M, Ohno Y, Maeda H. Results of surgical intervention for p-stage IIIA (N2) non-small cell lung cancer: acceptable prognosis predicted by complete resection in patients with single N2 disease with primary tumor in the upper lobe. J Thorac Cardiovasc Surg 2004;127:1100–1106.
[3] Saito M, Kato H. Prognostic factor in patients with pathological and N2 non-small cell lung cancer. Ann Thorac Cardiovasc Surg 2008;14:1–2.
[4] Riquet M, Assouad J, Bagan P, Foucault C, Le Pimpec Barthes F, Dujon A, Danel C. Skip mediastinal lymph node metastasis and lung cancer: a particular N2 subgroup with a better prognosis. Ann Thorac Surg 2005; 79:225–233.
[5] Kato H, editor. Classification of lung cancer, 1st English edition. Tokyo: The Japan Lung Cancer Society Kanehara & Co., Ltd., 2000.
[6] Sobin LH, Wittekind Ch, editors. UICC: TNM classification of malignant tumors, 5th edition. New York: John Wiley & Sons, 1997.
[7] Naruke T, Suemasu K, Ishikawa S. Lymph node mapping and curability at various levels of metastasis in resected lung cancer. J Thorac Cardiovasc Surg 1978;76:832–839.
[8] Peto R, Pike MC, Armitage P, Breslow NE, Cox DR, Howard SV, Mantel N, McPherson K, Peto J, Smith PG. Design and analysis of randomized clinical trials requiring prolonged observation of each patient. I. Introduction and design. Br J Cancer 1976;34:585–612.
[9] Prenzel KL, Mönig SP, Sinning JM, Baldus SE, Brochhagen HG, Schneider PM, Hölscher AH. Lymph node size and metastatic infiltration in non-small cell lung cancer. Chest 2003;123:463–467.
[10] Andre F, Grunenwald D, Pignon JP, Dujon A, Pujol JL, Brichon PY, Brouchet L, Quoix E, Westeel V, Chevalier TL. Survival of patients with resected N2 non-small-cell lung cancer: evidence for a subclassification and implications. J Clin Oncol 2000;18:2981–2989.
[11] Robinson LA, Wagner H Jr, Ruckdeschel JC. Treatment of stage IIIA non-small cell lung cancer. Chest 2003;123:202S–220S.
[12] Miyamoto H, Hata E, Sakao Y, Harada R, Hamada T. Evaluation of neck lymph node dissection and extended lymphadenectomy through a collar incision and median sternotomy for lung cancer. Jpn J Thorac Cardiovasc Surg 1995;16:1804–1809.
[13] Riquet M, Hidden G, Debesse B. Direct lymphatic drainage of lung segments to mediastinal nodes. J Thorac Cardiovasc Surg 1989;97:625–632.
[14] Casali C, Stefani A, Natali P, Rossi, G, Morandi U. Prognostic factors in surgically resected N2 non-small cell lung cancer: the importance of patterns of mediastinal lymph nodes metastasis. Eur J Cardiothorac Surg 2005;28:33–38.
[15] Izbicki JR, Passlick B, Pantel K, Pichlmeier U, Hosch SB, Karg O, Thetter O. Effectiveness of radical systematic mediastinal lymphadenectomy in patients with resectable non-small cell lung cancer. Ann Surg 1998; 227:138–144.

eComment: Stage IIIA-N2 non-small cell lung cancer: could a new scoring system improve the management of heterogeneous disease?

Authors: ***Filippo Lococo****, Department of General Thoracic Surgery, Catholic University of Rome, Rome, Italy;* ***Giovanni Leuzzi, Stefano Cafarotti, Stefano Margaritora***

doi:10.1510/icvts.2010.249896A

We read with great interest the article by Nakagiri et al. [1] and colleagues reporting their long-term results in the surgical treatment of pathological stage IIIA-N2 non-small cell lung cancer (NSCLC). The authors discuss the clinical validity of the lymph node metastasis sub-classification, seeking in particular to analyze some pathological findings (involvement of the highest mediastinal lymph node or not; 'skip' vs. 'non-skip' N2-disease; 'single N2' vs. 'multiple N2'; 'single station N2' vs. 'multiple station N2') that could have some potential impact on the survival. We completely concur with the statement that N2 disease is a mixture of heterogeneous prognostic subgroups, where different levels of involvement [it is appropriate to add also the number of lymph nodes invaded, lymph node ratio (invaded/total) [2] along with type of involvement (intra vs. extra capsular)] may indeed represent significantly different prognostic classes [3]. Despite this prognostic variability of the N2-disease, no revision was made in accordance with the International Association for the Study of Lung Cancer (IASLC) analysis of the N-descriptors in the 7th edition of the TNM classification for lung cancer ('there were insufficient data to determine whether the N-descriptors should be subdivided') [4]. Probably, instead of analyzing each prognostic factor, the realization of a scoring system of the N2-status that takes into account all of these prognostic factors mentioned above would be more useful. This score may be obtained from the result of the retrospective analysis of large pathological data sets and the subsequent confirmation by specific prospective trials; of course the ultimate goal of this score could be the identification of prognostic classes (e.g. N2a, N2b, N2c, etc.) in the clinical phase in order to facilitate the stage-dependent treatment planning and, consequently, the long-term outcomes of stage IIIa-N2. On the basis of these considerations, we warmly advocate further investigations of prognostic predictors in stage IIIa-N2 disease.

References

[1] Nakagiri T, Sawabata N, Funaki S, Inoue M, Kadota Y, Shintani Y, Okumura M. Validation of pN2 sub-classifications in patients with pathological stage IIIA N2 non-small cell lung cancer. Interact CardioVasc Thorac Surg 2011;12:733–738.
[2] Tanaka F, Yanagihara K, Otake Y, Kawano Y, Miyahara R, Takenaka K, Katakura H, Ishikawa S, Ito H, Wada H. Prognostic factors in resected pathologic (p-) stage IIIA-N2, non-small-cell lung cancer. Ann Surg Oncol 2004;11:612–618.
[3] Cerfolio RJ, Maniscalco L, Bryant AS. The treatment of patients with stage IIIa non-small cell lung cancer from N2 disease: who returns to the surgical arena and who survives. Ann Thorac Surg 2008;86:912–920.
[4] Rusch VW, Crowley J, Giroux DJ, Goldstraw P, Im JG, Tsuboi M, Tsuchiya R, Vansteenkiste J; International Staging Committee; Cancer Research and Biostatistics; Observers to the Committee; Participating Institutions. The IASLC Lung Cancer Staging Project: proposals for the revision of the N descriptors in the forthcoming seventh edition of the TNM classification for lung cancer. J Thorac Oncol 2007;2:603–612.

Published OnlineFirst December 14, 2010; DOI:10.1158/1541-7786.MCR-10-0340

Molecular Cancer Research

The Transmembrane Adaptor Cbp/PAG1 Controls the Malignant Potential of Human Non –Small Cell Lung Cancers That Have c-Src Upregulation

Takashi Kanou, Chitose Oneyama, Kunimitsu Kawahara, et al.

Mol Cancer Res 2011;9:103-114. Published OnlineFirst December 14, 2010.

Published OnlineFirst December 14, 2010; DOI:10.1158/1541-7786.MCR-10-034

Molecular Cancer Research

Signaling and Regulation

The Transmembrane Adaptor Cbp/PAG1 Controls the Malignant Potential of Human Non–Small Cell Lung Cancers That Have c-Src Upregulation

Takashi Kanou[1,2], Chitose Oneyama[1], Kunimitsu Kawahara[3], Akira Okimura[3], Mitsunori Ohta[4], Naoki Ikeda[4], Yasushi Shintani[2], Meinoshin Okumura[2], and Masato Okada[1]

Abstract

The tyrosine kinase c-Src is upregulated in various human cancers, although the precise regulatory mechanism underlying this upregulation is unclear. We previously reported that a transmembrane adaptor Csk-binding protein (Cbp; PAG1) plays an important role in controlling the cell transformation that is induced by the activation of c-Src. To elucidate the *in vivo* role of Cbp, we examined the function of Cbp in lung cancer cell lines and tissues. In this study, we found that Cbp was markedly downregulated in human non–small cell lung cancer (NSCLC) cells. The ectopic expression of Cbp suppressed the anchorage-independent growth of the NSCLC cell lines (A549 and Lu99) that had upregulated c-Src, whereas the Cbp expression had little effect on other NSCLC cell lines (PC9 and Lu65) that express normal levels of c-Src. The expression of Cbp suppressed the kinase activity of c-Src in A549 cells by recruiting c-Src and its negative regulator, C-terminal Src kinase (Csk), to lipid rafts. The treatment with Src inhibitors, such as PP2, dasatinib, and saracatinib, also suppressed the growth of A549 cells. Furthermore, Cbp expression attenuated the ability of A549 cells to form tumors in nude mice, invade *in vitro*, and metastasize *in vivo*. In addition, we found a significant inverse correlation between the level of Cbp expression and the extent of lymph node metastasis in human lung cancers. These results indicate that Cbp is required for the Csk-mediated inactivation of c-Src and may control the promotion of malignancy in NSCLC tumors that are characterized by c-Src upregulation. *Mol Cancer Res; 9(1); 103–14. ©2010 AACR.*

Introduction

Lung cancer is the leading cause of cancer death among elderly men and is the second leading cause of cancer death among elderly women in Japan. From 2000 to 2007, the mortality rate due to lung cancer among the elderly population was 272.41/100,000 and 62.45/100,000 in men and women, respectively (1). Previous reports have demonstrated that lung cancer development involves both environmental and genetic factors (2). Over the past few decades, the methods for the diagnosis and treatment of lung cancer have improved. Recently, targeted molecular therapy in the treatment for non–small cell lung cancer (NSCLC) has received significant attention. Although epidermal growth factor receptor (EGFR) inhibitors have been successfully developed, NSCLC patients still have unfavorable prognoses (3). Therefore, the development of novel therapeutic strategies for the treatment of NSCLC is urgently needed.

c-Src was the first identified proto-oncogene product, and extensive research has shown that c-Src plays crucial roles in various intracellular signaling pathways that are implicated in cell growth, adhesion, and migration (4, 5). Several reports have shown that the overexpression or hyperactivity of c-Src is common in human lung cancers, especially in adenocarcinomas (6–10); however, the *C-SRC* gene is rarely mutated in human cancers, and the involvement of c-Src protein expression or enzymatic activation in the etiology of human cancer remains obscure (11). The kinase activity of c-Src is tightly regulated by several factors. A critical protein that negatively regulates c-Src activation is C-terminal Src kinase (Csk), which phosphorylates the negative regulatory tyrosine residue of c-Src (Tyr529; refs. 12, 13). Csk expression has been reported to be reduced in hepatocellular carcinoma in comparison with normal tissue, and this alteration may be correlated with c-Src activation (14). These observations suggest that Csk has a tumor-suppressive activity and that its reduced expression may facilitate the malignant cell behavior that is promoted by c-Src; however, the mechanisms underlying the downregulation of Csk in cancer cells are unclear.

Authors' Affiliations: [1]Department of Oncogene Research, Research Institute for Microbial Diseases; [2]Department of General Thoracic Surgery, Osaka University Graduate School of Medicine, Osaka University, Suita; Departments of [3]Pathology and [4]Thoracic Surgery, Osaka Prefectural Medical Center for Respiratory and Allergic Diseases, Osaka, Japan

Corresponding Author: Masato Okada, Department of Oncogene Research, Research Institute for Microbial Diseases, Osaka University. 3-1 Yamada-oka, Suita, Osaka 565-0871, Japan. Phone: 81-6-6879-8297; Fax: 81-6-6879-8298. E-mail: okadam@biken.osaka-u.ac.jp

doi: 10.1158/1541-7786.MCR-10-0340

Published OnlineFirst December 14, 2010; DOI:10.1158/1541-7786.MCR-10-0340

Csk is a cytoplasmic protein (15), and, thus, it has been proposed that Csk requires an appropriate membrane adaptor protein to access the membrane-anchored c-Src. We and another group previously identified the Csk-binding protein (Cbp), which is also known as PAG1 (16), as a specific membrane adaptor of Csk (17). Cbp exclusively localizes in lipid rafts and is involved in regulating the activity of Src family kinases (SFK) through the recruitment of Csk to lipid rafts where SFKs accumulate (17, 18). Several recent studies have implicated Cbp in cancer progression. In colon cancer patients, Cbp expression was significantly downregulated in some tumors in comparison with adjacent normal tissues (19), suggesting that Cbp has a tumor suppressor function for some types of cancer; however, other studies have shown that Cbp is overexpressed in renal cell carcinoma (RCC) and serves as a positive regulator of tumor malignancy in RCC patients (20). Thus, it has been suggested that Cbp plays distinct roles in controlling tumor progression depending on the cancer type.

In this study, we investigated the function of Cbp in several human lung cancer cell lines and tissues to address the precise *in vivo* role of Cbp. We show that Cbp expression is significantly downregulated in NSCLC cells and that the overexpression of Cbp in NSCLC cells, in which c-Src is highly activated, results in the suppression of tumor growth by promoting Csk-mediated c-Src inactivation. In addition, we show that Cbp inhibits both the *in vitro* invasiveness and the *in vivo* metastasis of a NSCLC cell line, and that there is a significant correlation between the Cbp expression level and lymph node metastasis. These findings suggest that Cbp can suppress the malignant potentials of NSCLC by attenuating the c-Src–mediated tumorigenic pathway.

Materials and Methods

Cell lines and reagents

The human NSCLC cell lines (A549, PC9, PC10, Lu65, Lu99, Lc4a, Lc3, Lc2, Lc23, Lc28, EBC-1, and RERF-LC-MS) were kindly provided by Dr. K. Kodama and Dr. M. Yutsudo. Normal human lung cells (13Lu, 39Lu, and 888Lu) were obtained from the European Collection of Cell Cultures (ECACC). A549 cells were cultured in Dulbecco's modified Eagle's medium (DMEM) and all other cancer cells were cultured in RPMI1640 (Nacalai). In both cases, the medium was supplemented with 10% FBS. Normal lung cells were maintained in Eagle's minimum essential medium (EMEM; DS Pharma Biomedical) that was supplemented with 10% FBS and a 1% nonessential amino acids solution. PP2 (Calbiochem), Dasatinib (BioVision), and Saracatinib (BioVision) were solubilized in DMSO to obtain 10 to 20 mmol/L of stock solutions. Stock solutions were stored at −20°C and diluted in DMEM for each experiment.

Cancer specimens

NSCLC specimens and paired noncancerous tissues were snap-frozen in liquid nitrogen immediately after resection. The resected lung tissues were divided upon visual inspection into tumor (T) and nontumor (N) regions, which were then histologically confirmed. To compare the Cbp mRNA expression level in each NSCLC case, we used formalin-fixed, paraffin-embedded (FFPE) samples of human primary lung adenocarcinoma. Sections (10 μm) were cut from each block and placed in a 1.5-mL test tube. Total RNA was then extracted using the High Pure FFPE RNA Micro Kit (Roche). This study was approved by the ethical review board of the Osaka Prefectural Medical Center for Respiratory and Allergic Diseases.

Retroviral gene transfer and expression

All gene transfer and expression protocols were performed using previously described methods (21). Briefly, the cDNAs that encode wild-type human Cbp and its mutant, which had a substitution of Tyr314 to Phe (Y314F), were subcloned into the retroviral vectors pCX4puro and pCX4bleo, respectively. All constructs were generated using a PCR-based procedure. The retroviral vectors were transfected into Plat-E, which is an ecotropic murine leukemia virus-packaging cell line, using Fugene6 (Boehringer) according to the manufacturer's directions. To transfer the gene into human cells, we used pGP + pE-Ampho (Takara Bio), which is an amphotropic retrovirus-packaging construct. Infected cell populations were selected with puromycin or bleomycin, and the mixed cell populations were subjected to each assay that is described in this study.

Antibodies

We generated an anti-human Cbp antibody by immunizing rabbits with a GST-Cbp (residues 331–430) fusion protein. We acquired the anti-Src antibody (Ab-1) from Calbiochem; the anti-Src pY418, anti-Src pY529, and anti-FAK pY397 antibodies from Biosource; the anti-FAK, anti-Csk, and anti-β-tubulin antibodies from Santa Cruz Biotechnology; the anti-Caveolin antibody from BD Transduction Laboratories; the anti-Transferrin receptor from Zymed; and the anti-Akt, anti-Akt pS473, anti-Erk, and anti-Erk pT202/pY204 antibodies from Cell Signaling. Horseradish peroxidase (HRP)-conjugated anti-mouse or anti-rabbit IgG (Zymed) was used as the secondary antibody.

Western blot and immunoprecipitation

Cells were washed and lysed in ODG buffer (50 mmol/L of Tris-HCl, pH 7.4, 1 mmol/L of EDTA, 0.25 mol/L of NaCl, 20 mmol/L of NaF, 1 mmol/L of Na_3VO_4, 1% Nonidet P-40, 2% Octyl-D-glucoside, 5 mmol/L of β-mercaptoethanol, 0.1% aprotinin, 0.1% leupeptin, 1 mmol/L of PMSF, and 5% glycerol). Equal amounts of total protein were separated using SDS-PAGE and transferred onto nitrocellulose membranes. The membranes were blocked and probed with primary antibodies, followed by incubation with HRP-conjugated secondary antibodies. For immunoprecipitation, the precleared lysate (1-mg protein) was incubated with the indicated antibodies for 1 hour and protein G-Sepharose (GE Healthcare) for 3 hours at 4°C. The immunoprecipitates were washed with ODG buffer and analyzed by Western blotting.

Published OnlineFirst December 14, 2010; DOI:10.1158/1541-7786.MCR-10-0340

In vitro proliferation assay

In vitro anchorage-dependent growth was assessed by using an assay that is based on the cleavage of the tetrazolium salt WST-1 into formazan by cellular mitochondrial dehydrogenases (Roche). Each cancer cell line was plated in 96-well microplates at a density of 1,000 cells per well. Cells were allowed to grow for 72 hours, and 10 μL of WST-1 reagent was applied to each well followed by 1-hour incubation. The absorbance at 450 nm was read with a microplate reader, and the average of 3 wells was determined. Each experiment was repeated 3 times.

Soft agar assay

Single-cell suspensions of 1×10^4 cells in 1.5 mL of DMEM that contained 10% FBS and 0.36% agar were plated onto a layer of 2.5 mL of the same medium that contained 0.7% agar in 6-well culture dishes. Viable colonies were stained with MTT 10 to 14 days after plating. Colonies larger than approximately 0.1 mm in diameter were scored.

Invasion assay

Invasion assays were conducted using a BioCoat Matrigel Invasion Chamber (BD Bioscience) according to the manufacturer's instructions. A cell suspension (5×10^4 cells) in serum-free medium was added to the inserts, and each insert was placed in the lower chamber, which contained a culture medium that was supplemented with 10% FBS. After a 24-hour incubation, invasiveness was evaluated by staining the cells that migrated through the extracellular matrix layer.

Tumor growth and metastasis in nude mice

Female BALB/c athymic nude mice (4 weeks old) were purchased from Japan CLEA. Cancer cells were grown, harvested, washed with PBS, and resuspended in serum-free DMEM. For the analysis of tumor growth, 1×10^6 cancer cells (0.2 mL) were subcutaneously inoculated into nude mice. Tumor sizes were monitored weekly, and tumor volume was calculated on the basis of the following formula: volume $= 0.5 \times \text{length} \times (\text{width})^2$. For the lung metastasis model, 5×10^6 cells were intravenously injected into mice via the tail vein. After 1 month, mice were euthanized using diethyl ether, and the number of metastatic nodules was determined in lungs that were fixed in Bouin's solution (22). Mice were handled and maintained according to the Osaka University guidelines for animal experimentation.

Preparation of detergent-resistant membrane domains

The separation of detergent-resistant membrane domains (DRM) was performed as previously described (23). Briefly, cells were lysed in a buffer that contained 0.25% Triton X-100, and the lysate was placed at the bottom of a discontinuous sucrose gradient (40%/35%/5%). After centrifugation at 40,000 rpm for 6 hours, fractions were collected from the top of the gradient, and aliquots were analyzed by Western blotting. The separation of DRMs and non-DRMs was confirmed by detecting caveolin-1 and transferrin receptor (TFR) as markers for DRMs and non-DRMs, respectively.

Real-time quantitative PCR

Total RNA was extracted from cancer cell lines and frozen tissue samples using Sepasol (Nacalai). The High Pure FFPE RNA Micro Kit (Roche) was used to extract total RNA from the FFPE tissue samples. The Transcriptor First Strand cDNA Synthesis Kit (Roche) was used to reverse transcribe all samples for qPCR. The mRNA levels of Cbp (ID: 179693), matrix metalloproteinase (MMP)-2/9 (ID: 234422, 957562), and glyceraldehydes-3-phosphate dehydrogenase (GAPDH; ID: 99999915) were quantified using TaqMan gene expression assays (Applied Biosystems). PCR was performed using an Applied Biosystems 7900HT Fast Real-time PCR System and Sequence Detection System, Software v2.2.1. The expression of the target genes was normalized to that of *GAPDH*.

Immunohistochemistry

Cancer cells were cultured on fibronectin-coated plates and fixed with 4% PFA (paraformaldehyde) for 15 minutes at room temperature. After blocking with 1% BSA (bovine serum albumin), the cells were incubated with the primary antibodies overnight at 4°C. The cells were then incubated with secondary antibodies for 1 hour at room temperature, and coverslips were mounted on the glass slides. Alexa Fluor 488 phalloidin (Invitrogen) was used to stain the F-actin. Images were photographed using a fluorescent confocal microscope (Olympus, FV-1000). Immunohistochemistry was performed on FFPE tumor samples. Sections from cancerous and corresponding normal tissue were stained with an anti-Cbp antibody or a neutralized antibody. The detection of immunoreactivity was performed using an iVIEW DAB Detection Kit on Benchmark (Ventana Medical Systems).

Wound-healing assay

A549 cells were seeded into 6-well plates and incubated in a medium that was supplemented with 10% FBS until the cells reached confluence. The confluent monolayer cultures were then scratched with a pipette tip. After incubation for 24 hours, the wounded areas were examined with a light microscope and photographed. The wound gap distances were then measured. All experiments were performed in triplicate.

Results

Cbp expression is downregulated in NSCLC cells

As an initial experiment, we compared, by Western blotting, the expression levels of Cbp and c-Src proteins in normal lung cells and in a variety of NSCLC cells. As shown in Figure 1A, the expression of Cbp was markedly downregulated in NSCLC cells in comparison to those in normal lung cells. In contrast, the expression of c-Src varied depending on cell types; higher levels of c-Src expression

Published OnlineFirst December 14, 2010; DOI:10.1158/1541-7786.MCR-10-0340

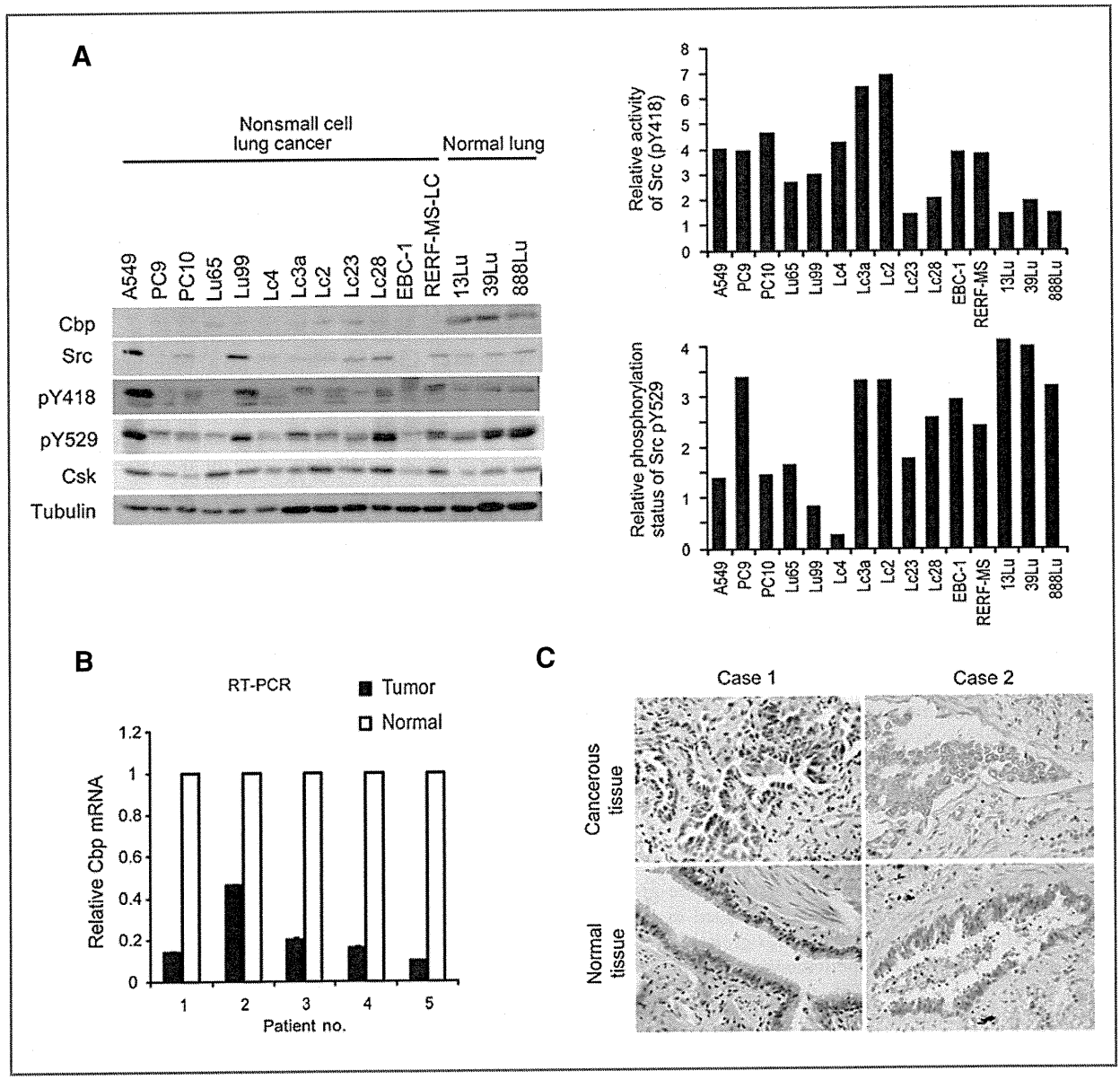

Figure 1. Cbp expression is downregulated in NSCLC cells. A, the protein expressions of Cbp, c-Src, phosphorylated c-Src (pY418 and pY529), and Csk in the indicated cell lines were assessed by Western blotting. Tubulin was used as the loading control (left). The ratio of signal intensity between total Src and pY418 (relative activity of Src; top right graph) or pY529 (relative phosphorylation status of Src pY529; bottom right graph) is shown. B, quantitative real-time (RT) PCR was performed using total RNA that was isolated from fresh frozen tissue samples. The relative levels of Cbp mRNA, which were normalized to GAPDH mRNA expression, in lung tumors (black bars) and matched normal tissues (white bars) are shown. C, immunohistochemical staining was performed for Cbp in lung tissues. Sections of cancerous tissue and normal tissue were stained with anti-Cbp and eosin and observed using light microscopy at 400× magnification.

were detected in A549 and Lu99 cells. These suggest that the expression level of Cbp is not necessarily correlated with the level of c-Src. However, the majority of NSCLC cells exhibited a higher ratio of the signal intensity of pY418 (an autoactivation site) to that of total Src protein (Fig. 1A, top right) than normal cells. In addition, the phosphorylation status of pY529 (a negative regulatory site that is phosphorylated by Csk) in several NSCLC cells was lower than that in normal cells (Fig. 1A, bottom right). These observations demonstrate that c-Src is widely activated in NSCLC cells, although the expression of Csk in NSCLC cells is similar to that in normal lung cells (Fig. 1A, left).

To examine whether Cbp expression was altered in human cancer tissues, the expression of Cbp mRNA in frozen samples from 4 pairs of NSCLC tissues and their matched noncancerous control tissues was analyzed by

Published OnlineFirst December 14, 2010; DOI:10.1158/1541-7786.MCR-10-0340

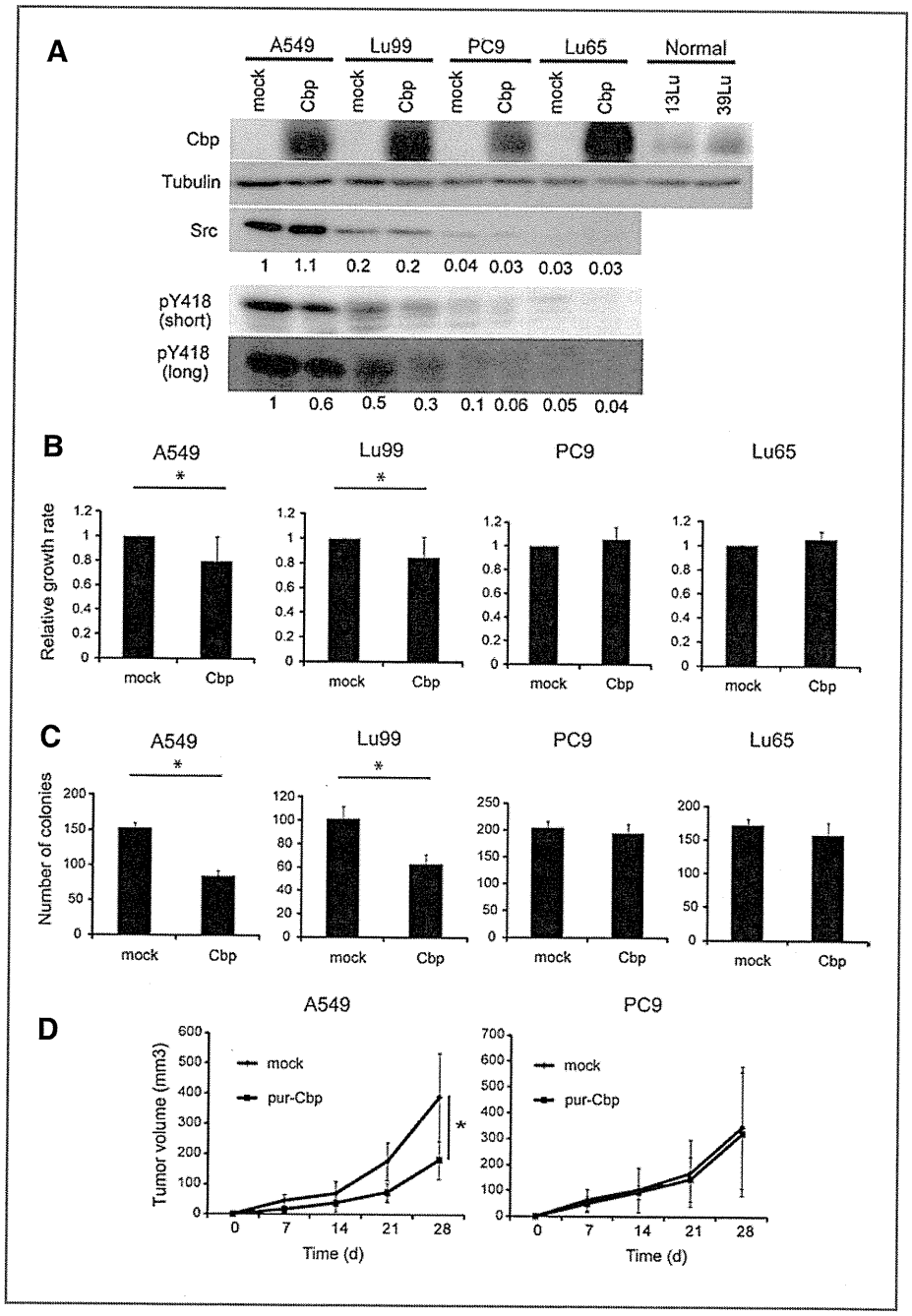

Figure 2. The ectopic expression of Cbp inhibits the activation of c-Src and the proliferative potential of lung cancer cells. A, total cell lysates from control and Cbp-expressing A549, Lu99, PC9, and Lu65 cells and normal lung cells were analyzed by Western blotting with the indicated antibodies. The depicted values reflect the fold changes in signal intensity of the total c-Src and pY418 from 2 independent experiments, which are normalized to the signal intensities of A549 mock cells. B, anchorage-dependent growth was assessed by an *in vitro* proliferation assay using WST-1. The relative absorbance (mean ± SE) in Cbp-expressing cells in comparison to that in mock cells was obtained from 3 independent experiments. C, anchorage-independent growth was examined by a colony formation assay in soft agar. Colonies were stained with MTT 14 days after plating. The colony numbers per cm^2 (mean ± SE) that were obtained from 3 independent experiments are shown. Student's *t* tests: *, $P < 0.05$. D, the ability of tumor formation was examined in a mouse xenograft model. Cells (1×10^6) were subcutaneously inoculated into nude mice. The tumor volumes (mm^3; mean ± SE) that were obtained from 4 mice in each group are plotted as a function of days after inoculation. *, $P < 0.05$.

quantitative real-time PCR. The expression of Cbp mRNA was significantly downregulated in all human lung cancer samples in comparison to that in their adjacent normal controls (Fig. 1B). Immunohistochemistry also indicated that the tumor cells very weakly expressed the Cbp protein, although the Cbp protein was readily detectable in the normal bronchiolar epithelia (Fig. 1C). These results indicate that Cbp expression is generally downregulated in NSCLC cells as well as in NSCLC tissues.

The ectopic expression of Cbp inhibits anchorage-independent growth and tumor growth of NSCLC cells in which c-Src is upregulated

To investigate the role of Cbp downregulation in NSCLC cells, we ectopically expressed Cbp in A549, Lu99, PC9, and Lu65 cells; A549 and Lu99 cells have the highest levels of c-Src upregulation, whereas PC9 and Lu65 cells express normal levels of c-Src. The expression levels of Cbp in the transfected cells substantially exceeded those in the normal lung cells (Fig. 2A); however, because

Published OnlineFirst December 14, 2010; DOI:10.1158/1541-7786.MCR-10-0340

the A549 and Lu99 cells exhibited a marked (>10-fold) upregulation of the c-Src protein in comparison to normal lung cells (Fig. 1A), the ratio of overexpressed Cbp to c-Src in these cells appeared to be at a comparable level to that in normal cells. Western blot analysis revealed that the phosphorylation of c-Src Tyr418 in all 4 cell lines was suppressed by the overexpression of Cbp; although, the levels of total c-Src and pY418 in PC9 and Lu65 cells were much lower than those in A549 cells (Fig. 2A). These results indicate that the kinase activity of c-Src is inhibited by the expression of Cbp in these cells.

We next examined the effects of Cbp expression on the growth ability of these NSCLC cells. In A549 and Lu99 cells, the expression of Cbp significantly suppressed both anchorage-dependent and anchorage-independent growth, as assessed by a growth assay and a soft agar colony formation assay (Fig. 2B and C); however, in PC9 and Lu65 cells, the expression of Cbp had little effect on both anchorage-dependent growth and anchorage-independent growth. The suppressive effect of Cbp on tumor growth was further examined in a xenograft mouse model. Nude mice were subcutaneously injected with Cbp-overexpressing A549 and PC9 cells or control cells, and tumor formation was monitored weekly. Similar to anchorage-independent growth, the expression of Cbp significantly suppressed the tumor growth of A549 cells but not PC9 cells (Fig. 2C). These data suggest that Cbp can suppress the tumor growth of NSCLC cells, which have upregulated c-Src.

The Cbp-mediated suppression of tumor growth signaling is associated with a reduction in active c-Src in non–raft compartments.

To elucidate the molecular mechanisms by which Cbp suppresses tumor growth, we investigated the activity status of several Src downstream molecules, including FAK, Akt, and Erk, in A549 cells. Despite the reduction of total c-Src activity in these cells (Fig. 2A), the expression of Cbp preferentially suppressed the activity of FAK (pY379), whereas the activities of Akt and Erk were unchanged (Fig. 3A). To address the mechanism for the inactivation of FAK, we examined the membrane distribution of c-Src, FAK, and Csk by separating DRMs, in which major components of lipid rafts are concentrated (24). In Cbp-expressing cells, Cbp was enriched in the DRMs (Fig. 3B, right), representing its preferential localization to lipid rafts. In these cells, the activity of c-Src (pY418 signals) was substantially reduced in the non-DRMs, whereas the level of inactive c-Src (pY529) rather increased (Fig. 3B). Quantitative analysis revealed that the ratio of active c-Src (pY418) in the DRMs to that in the non-DRMs significantly increased in Cbp-expressing cells (Fig. 3C, left), whereas the levels of inactive c-Src (pY529) in the DRMs decreased (Fig. 3C, right). These findings demonstrate that the expression of Cbp can induce not only the suppression of c-Src activity but also the accumulation of active c-Src in lipid rafts. Consistent with the reduction of c-Src activity in the non-DRMs, the activity of FAK (pY397) that is present in the non-DRMs was appreciably suppressed (Fig. 3B). This raises the possibility that the Cbp-mediated elimination of active c-Src from the non–raft compartments may interfere with the access of active c-Src to FAK, which is crucial for tumor growth (18).

Cbp-Csk association and inhibition of c-Src activity are involved in the growth suppression of A549 cells

To further elucidate the mechanisms for the suppression of c-Src activity by the expression of Cbp, we examined the interaction between c-Src, Csk, and Cbp in A549 cells. Figure 3B demonstrates that Csk was detected in the DRMs from Cbp-expressing cells but was absent in the DRMs from the mock-treated cells. These data indicate that a part of Csk can be recruited to lipid rafts by the expression of Cbp. The immunoprecipitation assays for Cbp and c-Src revealed that Cbp coimmunoprecipitated with both c-Src and Csk (Fig. 4A), indicating that Cbp, Csk, and c-Src are able to form a ternary complex in lipid rafts. These results suggest that active c-Src and Csk are recruited to Cbp, which allows for an efficient inactivation of c-Src by Csk. To verify the importance of the formation of the Cbp-Csk complex in c-Src–induced tumor growth, we expressed a Cbp mutant (Cbp Y314F) with a mutation in the Csk-binding site in A549 cells; the mutant was expressed at a level that was comparable to that of wild-type Cbp (Fig. 4B). The expression of Cbp Y314F failed to suppress anchorage-independent growth in soft agar and tumor formation in a xenograft model (Fig. 4B and C), indicating that Cbp-Csk association is crucial for the tumor-suppressing effect of Cbp.

To examine whether the effects of Cbp expression on cell growth were mediated through suppressing c-Src activity, we further investigated the effects of Src inhibitors, including PP2, Dasatinib, and Saracatinib, on the growth of A549 cells. As shown in Figure 4D, the addition of each inhibitor decreased the phosphorylation levels of c-Src Tyr418. Consistent with the activity status of c-Src, the Src inhibitors dose dependently repressed both anchorage-dependent and anchorage-independent growth of these cells, as assessed by a growth assay and a soft agar colony formation assay (Fig. 4E and F). These data demonstrate that the upregulation of c-Src activity is indeed involved in the enhanced growth ability of A549 cells and suggest that the inhibition of c-Src by the Cbp-Csk regulatory circuit can also contribute to the suppression of tumor growth of A549 cells.

The expression of Cbp affects the cytoskeletal organization and motility of lung cancer cells

We next examined the effects of Cbp expression on the organization of the actin cytoskeleton because the actin cytoskeleton is crucial for regulating the invasion and metastasis of cancer cells (25). Although the control A549 cells had prominent actin stress fibers, Cbp expression substantially attenuated stress fiber formations (Fig. 5A). As detected by a wound-healing assay, cell motility was significantly repressed by Cbp expression (Fig. 5B). In

Published OnlineFirst December 14, 2010; DOI:10.1158/1541-7786.MCR-10-0340

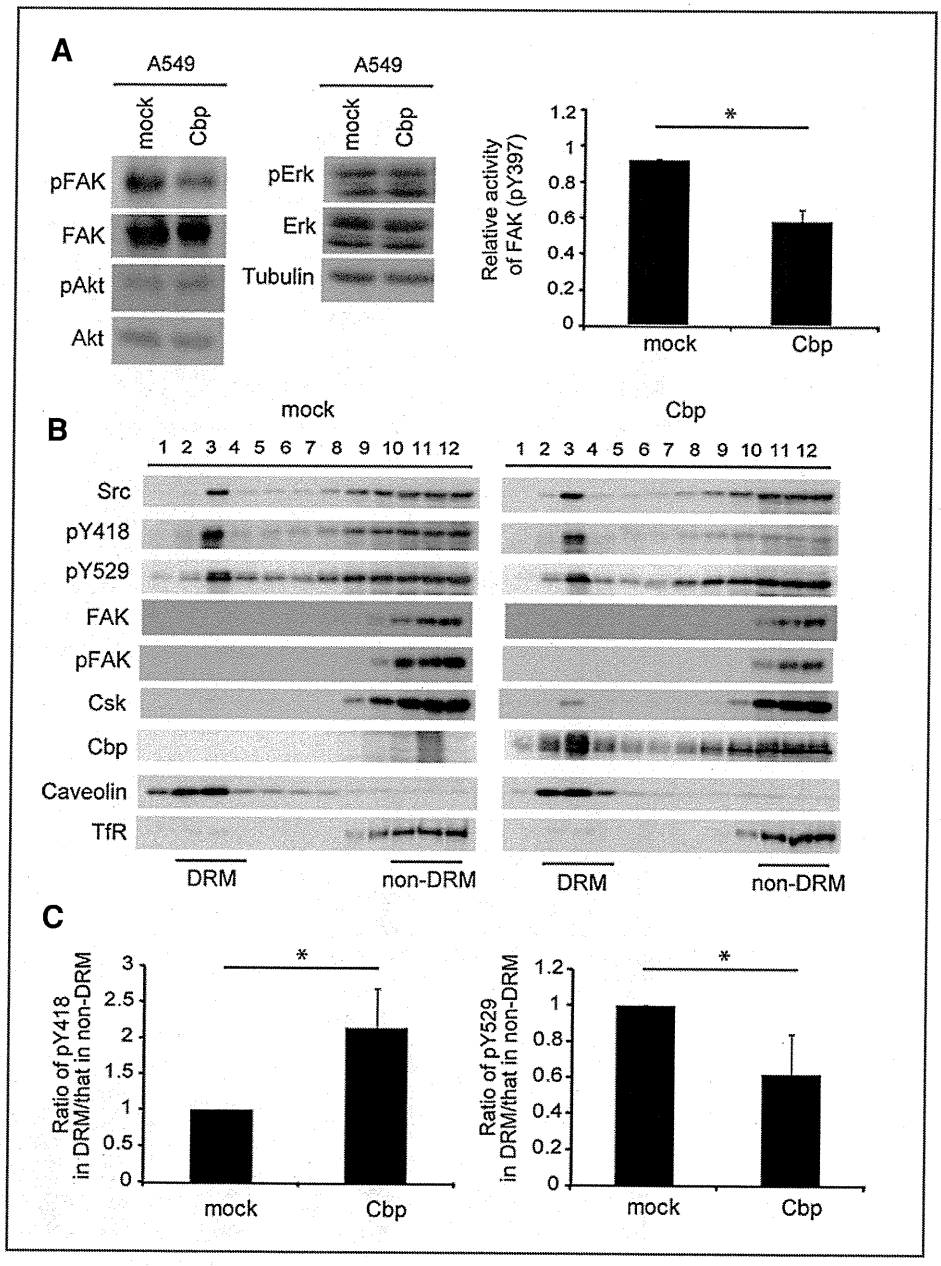

Figure 3. Cbp suppresses Src signaling by sequestering active c-Src into DRMs. A, total cell lysates from mock and Cbp-expressing A549 cells were analyzed by Western blotting with the indicated antibodies (left). The activity status of FAK was assessed by quantifying the relative intensity of the signal for phosphorylated forms in comparison to that of the nonphosphorylated forms. Relative specific activities (mean ± SE) of FAK in Cbp-expressing cells in comparison to those in mock cells were obtained from 3 independent experiments. B, DRMs and non-DRMs were separated from mock cells and Cbp-expressing cells, and each fraction was analyzed by Western blotting with the indicated antibodies. Caveolin 1 and TFR were detected as markers of DRMs and non-DRMs, respectively. C, the intensity of signals for Src pY418 (left) and pY529 (right) was quantified, and the ratios of the signals in DRMs to those in non-DRMs were compared between mock cells and Cbp-expressing cells. The relative values (mean ± SE) that were obtained from 3 independent experiments are shown.

contrast, the expression of Cbp Y314F had little effect on both the actin cytoskeleton and cell motility (Fig. 5A and B), indicating that the Cbp-Csk association and c-Src activity are crucial for controlling these cellular functions as well. The significant reduction in the invasiveness that is associated with Cbp expression was also observed in a Matrigel invasion assay (Fig. 5C). We further examined the expression of invasion-related metalloproteases (MMP-2, MMP-9), which degrade extracellular matrices. The expression of MMP-9 was significantly reduced in Cbp-expressing cells compared with control cells, whereas the expression of MMP-2 was only moderately repressed (Fig. 5D). These results suggest that Cbp can suppress the invasive potential of lung cancer cells by modulating cytoskeletal organization, cell motility, and the expression of MMPs via the inhibition of a c-Src–mediated pathway (5).

The expression of Cbp affects the metastatic ability of lung cancer cells

The observations that Cbp may control the invasive potential of lung cancer cells *in vitro* directed us to examine the suppressive role of Cbp in tumor metastasis *in vivo*.